

## Fluid and kinetic modeling of runaway electron generation from tritium beta decay and Compton scattering

I. Ekmark<sup>1</sup>, M. Hoppe<sup>2</sup>, T. Fülöp<sup>1</sup>, R.A. Tinguely<sup>3</sup>, R. Sweeney<sup>4</sup>,  
P. Jansson<sup>5</sup>, L. Antonsson<sup>1</sup>, O. Vallhagen<sup>1</sup> and I. Pusztai<sup>1</sup>

<sup>1</sup>Department of Physics, Chalmers University of Technology, Göteborg, Sweden.

<sup>2</sup>Department of Electrical Engineering, KTH Royal Inst. Technology, Stockholm, Sweden.

<sup>3</sup>Plasma Science and Fusion Center, Massachusetts Inst. Technology, Cambridge, MA, USA.

<sup>4</sup>Commonwealth Fusion Systems, Devens, MA, USA.

<sup>5</sup>Department of Computer Science and Engineering, Chalmers Univ. Technology, Göteborg, Sweden.

Runaway electrons (REs) can be generated during tokamak disruptions and pose a critical challenge for future tokamaks. Accurate modelling of the primary generation mechanisms is crucial, due to the sensitivity of avalanche multiplication to the initial seed of REs. For this reason, we derive kinetic sources of energetic electrons from tritium beta decay and Compton scattering [1]. These kinetic models are then compared to well established fluid models for RE generation [2] through simulations of a SPARC primary reference discharge [3] scenario where the seed generation is dominated by the activated RE generation mechanisms.

**Tritium beta decay** The kinetic source due to tritium beta decay can be derived using the energy spectrum for beta electrons [4]  $f_\beta(W) \propto F(p, 2)p\mathcal{W}(W_{\max} - W)^2$  for  $W \leq W_{\max}$ . Here  $\mathcal{W} = m_e c^2 \gamma$  is the total electron energy,  $W = m_e c^2 (\gamma - 1)$  is the electron kinetic energy,  $\gamma = \sqrt{p^2 + 1}$  is the Lorentz factor and  $p$  is the momentum normalized to  $m_e c$ . Since the maximum electron kinetic energy  $W_{\max} = 18.6 \text{ keV} \ll m_e c^2 = 511 \text{ keV}$ , we may take the non-relativistic limit of the Fermi function [5],  $F(p, Z_f) = 2\pi\alpha Z_f / [\beta(1 - \exp(-2\pi\alpha Z_f/\beta))]$ , with the normalized speed  $\beta = p/\gamma$ , the charge of the final state nucleus  $Z_f = 2$ , and the fine structure constant  $\alpha \approx 1/137$ . The emission angle of electrons during the decay is assumed to be random and uniformly distributed. Therefore, the source can be assumed to be isotropic in pitch angle, and we may write

$$4\pi p^2 dp \left( \frac{df}{dt} \right)_T = dW f_\beta(W) \implies \left( \frac{df}{dt} \right)_T = \frac{m_e c^2 \beta}{4\pi p^2} f_\beta(W) \propto \frac{1}{p^2} \frac{p\gamma(\gamma_{\max} - \gamma)^2}{1 - \exp[-4\pi\alpha/\beta]}. \quad (1)$$

This source integrated over the entire momentum space should yield the tritium decay rate, i.e.

$$\left( \frac{df}{dt} \right)_T = \frac{1}{C} \frac{\ln 2}{4\pi} \frac{n_T}{\tau_T} \frac{1}{p^2} \frac{p\gamma(\gamma_{\max} - \gamma)^2}{1 - \exp(-4\pi\alpha/\beta)}, \quad C = \int_0^{p_{\max}} \frac{1}{p^2} \frac{p\gamma(\gamma_{\max} - \gamma)^2}{1 - \exp(-4\pi\alpha/\beta)} p^2 dp, \quad (2)$$

where the half-life for tritium  $\tau_T \approx 12$  years and  $p_{\max}$  is the momentum corresponding to  $W_{\max}$ .

**Compton scattering** The Compton scattering process is described by the Klein-Nishina differential cross-section

$$\frac{d\sigma}{d\Omega} = \frac{r_e^2}{2} \frac{W_\gamma'^2}{W_\gamma^2} \left[ \frac{W_\gamma}{W_\gamma'} + \frac{W_\gamma'}{W_\gamma} - \sin^2(\theta) \right], \quad (3)$$

where  $r_e$  is the classical electron radius. Using the kinematic relation between the photon energy  $W_\gamma$ , the electron kinetic energy  $W$  and deflection angle  $\theta$  of the scattered photon, we can write

$$\cos\theta = 1 - m_e c^2 W / (W_\gamma W_\gamma'), \quad (4)$$

where  $W_\gamma' = W_\gamma - W$  is the scattered photon energy. This source can also be assumed to be

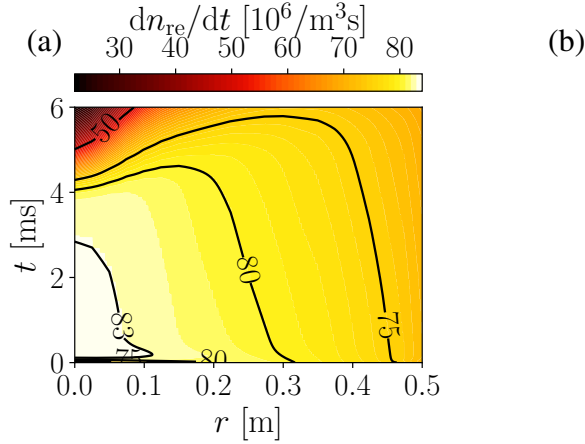


Figure 1: The kinetic sources from (a) tritium beta decay and (b) Compton scattering, integrated from  $p_c$  according to equation (7), are plotted as colored (and filled) contours, as functions of radius and time. On top of these are the fluid generation rates plotted as contour lines.

isotropic, since gamma photons will be emitted from the walls and enter the plasma from all sides in a nearly isotropic manner. Thus, in a plasma with total electron density  $n_{e,\text{tot}}$ , including both free and bound electrons, we can write

$$4\pi p^2 dp \left( \frac{df}{dt} \right)_C = n_{e,\text{tot}} \int_{W_{\gamma 0}}^{\infty} dW_{\gamma} \left[ \Gamma_{\gamma}(W_{\gamma}) \left( 2\pi \sin \theta \frac{d\sigma}{d\Omega} \right) d\theta(W, W_{\gamma}) \right], \quad (5)$$

where  $\Gamma_{\gamma}$  is the photon energy spectrum and the lower integration limit can be derived from (4) as  $W_{\gamma 0} = (p + \gamma - 1)/2$ . Thus the energetic electron source rate from Compton scattering

$$\left( \frac{df}{dt} \right)_C = \frac{n_{e,\text{tot}}}{2} \frac{1}{p^2} \int_{W_{\gamma 0}}^{\infty} dW_{\gamma} \Gamma_{\gamma}(W_{\gamma}) \frac{d\sigma}{d\Omega} \frac{\beta}{(W_{\gamma}/m_e c^2 + 1 - \gamma)^2}, \quad (6)$$

where we have used  $d\theta/dp = \beta / [\sin \theta (W_{\gamma}/m_e c^2 + 1 - \gamma)^2]$ .

Both kinetic sources are consistent with the fluid sources presented in [2], since

$$\left( \frac{dn_{re}}{dt} \right)_T = \ln 2 \frac{n_T}{\tau_T} \int_{W_c}^{W_{\text{max}}} f_{\beta}(W) dW = \int_{p > p_c}^{p < p_{\text{max}}} d^3 p \left( \frac{df}{dt} \right)_T, \quad (7a)$$

$$\left( \frac{dn_{re}}{dt} \right)_C = n_e^{\text{tot}} \int_{W_{\gamma 0}}^{\infty} \Gamma_{\gamma}(W_{\gamma}) \int_{\theta_c}^{\pi} \frac{d\sigma}{d\Omega} d\Omega dW_{\gamma} = \int_{p > p_c} d^3 p \left( \frac{df}{dt} \right)_C, \quad (7b)$$

where  $W_c$  is the energy and  $\theta_c$  the deflection angle corresponding to the critical momentum  $p_c$ . This was also confirmed by running SPARC simulations with the kinetic and the fluid sources and comparing the generation above the critical momentum. As shown in figure 1, the integrated kinetic sources and the fluid rates agree well in both values and contour shapes.

**Simulation setup** To compare the derived kinetic activated sources with the fluid sources derived in [2], we have performed reduced kinetic simulations with the DREAM code [6]. We have considered three cases – a case without any generation from the activated sources, a case with the fluid activated sources and a case with the kinetic activated sources.

All simulations treat the hot electrons ( $p \sim p_c$ ) kinetically, while the cold bulk electrons ( $p \ll p_c$ ) and the REs ( $p \gg p_c$ ) are treated as fluids. Such division of the electrons into three